Dephosphorylation of neural wiring protein shootin1 by PP1 phosphatase regulates netrin-1-induced axon guidance

Ria Fajarwati Kastian[1,2] [iD], **Kentarou Baba**[1], **Napol Kaewkascholkul**[1], **Hisashi Sasaki**[1], **Rikiya Watanabe**[3] [iD], **Michinori Toriyama**[1] [iD], and **Naoyuki Inagaki**[1,*]

From the [1]Laboratory of Systems Neurobiology and Medicine, Division of Biological Science, Nara Institute of Science and Technology, Ikoma, Nara, Japan; [2]Mammalian Cell Engineering and Signal Transduction Research Group, Research Center for Genetic Engineering, National Research and Innovation Agency, KST Soekarno, Bogor, West Java, Indonesia; [3]Molecular Physiology Laboratory, Cluster for Pioneering Research, RIKEN, Wako, Saitama, Japan

Reviewed by members of the JBC Editorial Board. Edited by Roger Colbran

Axon pathfinding is an essential step in neuronal network formation. Shootin1a is a clutch-linker molecule that is mechanically involved in axon outgrowth and guidance. It was previously shown that concentration gradients of axon guidance molecule netrin-1 in the extracellular environment elicit asymmetrically localized Pak1 kinase–mediated phosphorylation of shootin1a within axonal growth cones, which is higher on the netrin-1 source side. This asymmetric phosphorylation promotes shootin1a-mediated local actin–adhesion coupling within growth cones, thereby generating directional forces for turning the growth cone toward the netrin-1 source. However, how the spatial differences in netrin-1 concentration are transduced into the asymmetrically localized signaling within growth cones remains unclear. Moreover, the protein phosphatases that dephosphorylate shootin1a remain unidentified. Here, we report that protein phosphatase-1 (PP1) dephosphorylates shootin1a in growth cones. We found that PP1 overexpression abolished the netrin-1-induced asymmetric localization of phosphorylated shootin1a as well as axon turning. In addition, we show PP1 inhibition reversed the asymmetrically localized shootin1a phosphorylation within growth cones under netrin-1 gradient, thereby changing the netrin-1-induced growth cone turning from attraction to repulsion. These data indicate that PP1-mediated shootin1a dephosphorylation plays a key role in organizing asymmetrically localized phosphorylated shootin1a within growth cones, which regulates netrin-1-induced axon guidance.

During development of the nervous system, axons navigate to their appropriate synaptic targets with precision. The tip of the extending axons bears an exquisitely sensitive chemosensory and motile structure, the growth cone (1–4), which can sense subtle spatial differences in chemical cues of the microenvironment (5, 6) and produce forces for axon outgrowth (7–9) and guidance (10, 11). In addition, growth cones can navigate through heterogenous environments where the basal concentration of a chemical cue varies.

Netrin-1 is one of the best-characterized axon guidance molecules (12–14). Gradients of netrin-1 in the extracellular environment elicit growth cone attraction in vitro (13, 15). Knockout mice for netrin-1 or its receptor deleted in colorectal cancer shows impaired projection and guidance of axons in the ventral spinal and forebrain commissures (16–18).

Concerning forces for axon outgrowth and guidance, actin filaments (F-actins) polymerize at the leading edge of growth cones and depolymerize proximally, thereby resulting in inwardly directed F-actin retrograde flow (19, 20). Mechanical coupling between the F-actin retrograde flow and adhesive substrates by a clutch-linker molecule is thought to generate force for axon outgrowth (21–23). The clutch coupling produces traction forces on adhesive substrates and concurrently reduces the speed of the F-actin retrograde flow (21–23), thus converting actin polymerization into force that pushes the leading-edge membrane forward (24).

Shootin1a is a clutch-linker molecule involved in axon outgrowth (25) and guidance (10, 11). Shootin1a mechanically couples F-actin retrograde flow and adhesive substrates through its interactions with the actin-binding protein cortactin (26) and the cell adhesion molecule L1-CAM (11, 25). In addition, stimulation of deleted in colorectal cancer by netrin-1 activates signaling pathways, including Rac1, Cdc42, and their downstream kinase Pak1 in growth cones (27–31), which in turn induce Pak1-mediated shootin1a phosphorylation at Ser101 and Ser249 (23). The shootin1a phosphorylation enhances shootin1a–cortactin and shootin1a–L1-CAM interactions, resulting in the facilitation of the traction force for axon outgrowth (11, 26). We recently reported that a shallow gradient (0.4%) of extracellular netrin-1 that covers growth cones elicits asymmetrically localized Pak1-mediated shootin1a phosphorylation, which is higher on the netrin-1 source side (11). This in turn promotes local clutch coupling in growth cones, thereby generating directional forces that turn growth cone toward the netrin-1 source. Consistently, mice lacking shootin1a display abnormal projection of forebrain commissural axons, a phenotype similar to that of netrin-1 knockout mice (11).

Although these data indicate that Pak1 phosphorylates shootin1a and mediates netrin-1–induced axon guidance, the phosphatases that dephosphorylate shootin1a remain unidentified. Furthermore, elucidating how spatial differences in environmental cues are transduced into asymmetrically localized signaling within growth cones is key to understanding the basic principle of axon guidance. Protein phosphatase-1 (PP1) is a major protein serine/threonine phosphatase that is expressed ubiquitously in multiple subcellular regions of various eukaryotic cells (32–36) and plays key roles in the regulation of neuronal cytoskeletons and axon guidance (37, 38). Here, we report that PP1 dephosphorylates shootin1a at Ser101 and Ser249. Moreover, our data demonstrate that PP1-mediated shootin1a dephosphorylation plays a key role in organizing asymmetrically localized phosphorylated shootin1a within growth cones, which is required for netrin-1–induced attractive axon guidance.

Results

PP1 dephosphorylates shootin1a at Ser101 and Ser249

To identify the protein phosphatases that dephosphorylate shootin1a at Ser101 and Ser249, we focused on the three major neuronal serine/threonine protein phosphatases, PP1, PP2A, and PP2B (calcineurin) (38). First, we examined the effects of the phosphatase inhibitors: calyculin A (PP1/PP2A inhibitor), okadaic acid (PP1/PP2A inhibitor), fostriecin (PP2A inhibitor), FK506 (PP2B inhibitor), and tautomycetin (PP1 inhibitor). Application of 200 nM calyculin A or 100 nM okadaic acid to day *in vitro* 3 (DIV3) cultured mouse cortical neurons for 1 h significantly increased phosphorylated shootin1a at Ser101 (pSer101) and at Ser249 (pSer249) (Fig. 1). Tautomycetin is a selective phosphatase inhibitor for PP1 and specifically inhibits PP1 at 10 nM (39, 40). Tautomycetin at 10 nM significantly increased the levels of shootin1a phosphorylated at both sites (Fig. 1) as well as the phosphorylation of the control PP1 substrate, Ser10 of histone H3 (41) (Fig. S1*A*). However, treatments with fostriecin (10 nM) or FK506 (50 nM) did not affect the levels of phosphorylated shootin1 (Fig. 1), thereby raising the possibility that PP1 dephosphorylates shootin1a in hippocampal neurons.

To examine whether PP1 directly dephosphorylates shootin1a, we performed an *in vitro* phosphatase assay using purified phosphorylated shootin1a. Phosphorylated shootin1a was purified by immunoprecipitation from calyculin A-treated HEK293T cells expressing shootin1a (Fig. S1*B*), and then incubated with the catalytic subunit of PP1 or PP2A. As shown in Figure 2*A*, PP1 at 1.5 mU/μl completely dephosphorylated
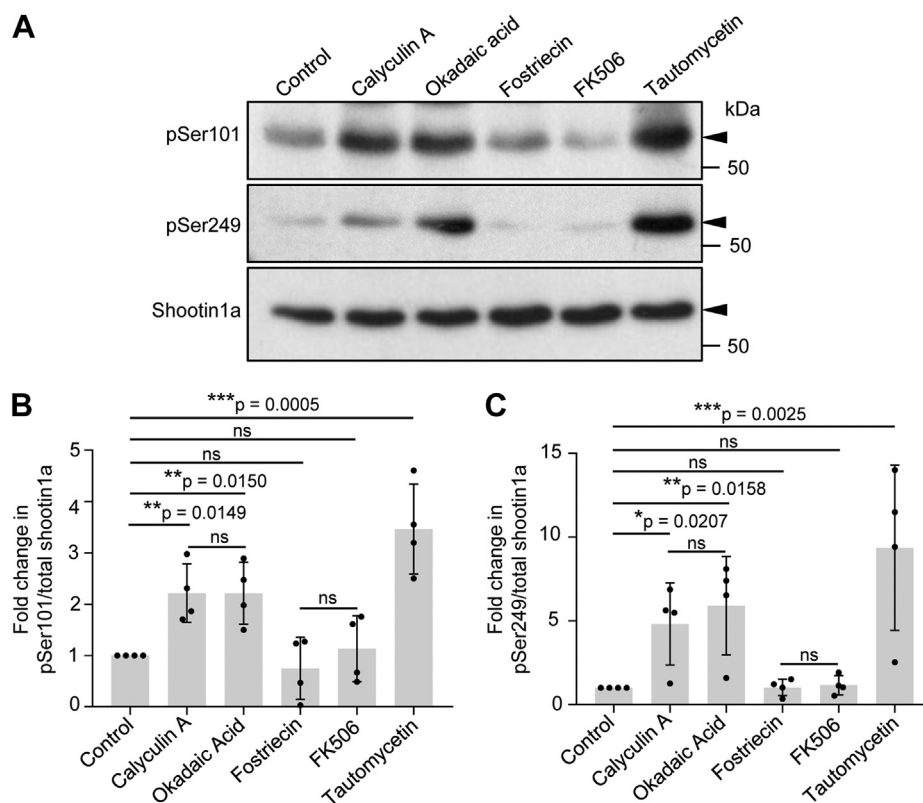

Figure 1. Inhibition of PP1 increases phosphorylated shootin1a in cultured neurons. *A*, cultured cortical neurons (DIV3) were treated with various phosphatase inhibitors: DMSO as a control, 200 nM calyculin A, 100 nM okadaic acid, 10 nM fostriecin, 50 nM FK506, or 10 nM tautomycetin. Protein lysates were prepared after 1 h treatment and analyzed by immunoblot with antibodies against pSer101, pSer249, and shootin1a. The full-length images for immunoblots are presented in Fig. S4. The graphs show quantitative analyses of phosphorylated shootin1a at Ser101 (*B*) and Ser249 (*C*), represented as the fold change relative to control neurons (N = 4). *B*: F (5, 18) = 11.33, $p < 0.00001$. *C*: F (5, 18) = 7.158, $p = 0.0008$. Data represent means ± SD; ***$p < 0.01$; **$p < 0.02$; *$p < 0.05$; ns, not significant (One-way ANOVA with Tukey`s multiple comparison test). DIV, day *in vitro*; PP1, protein phosphatase-1.
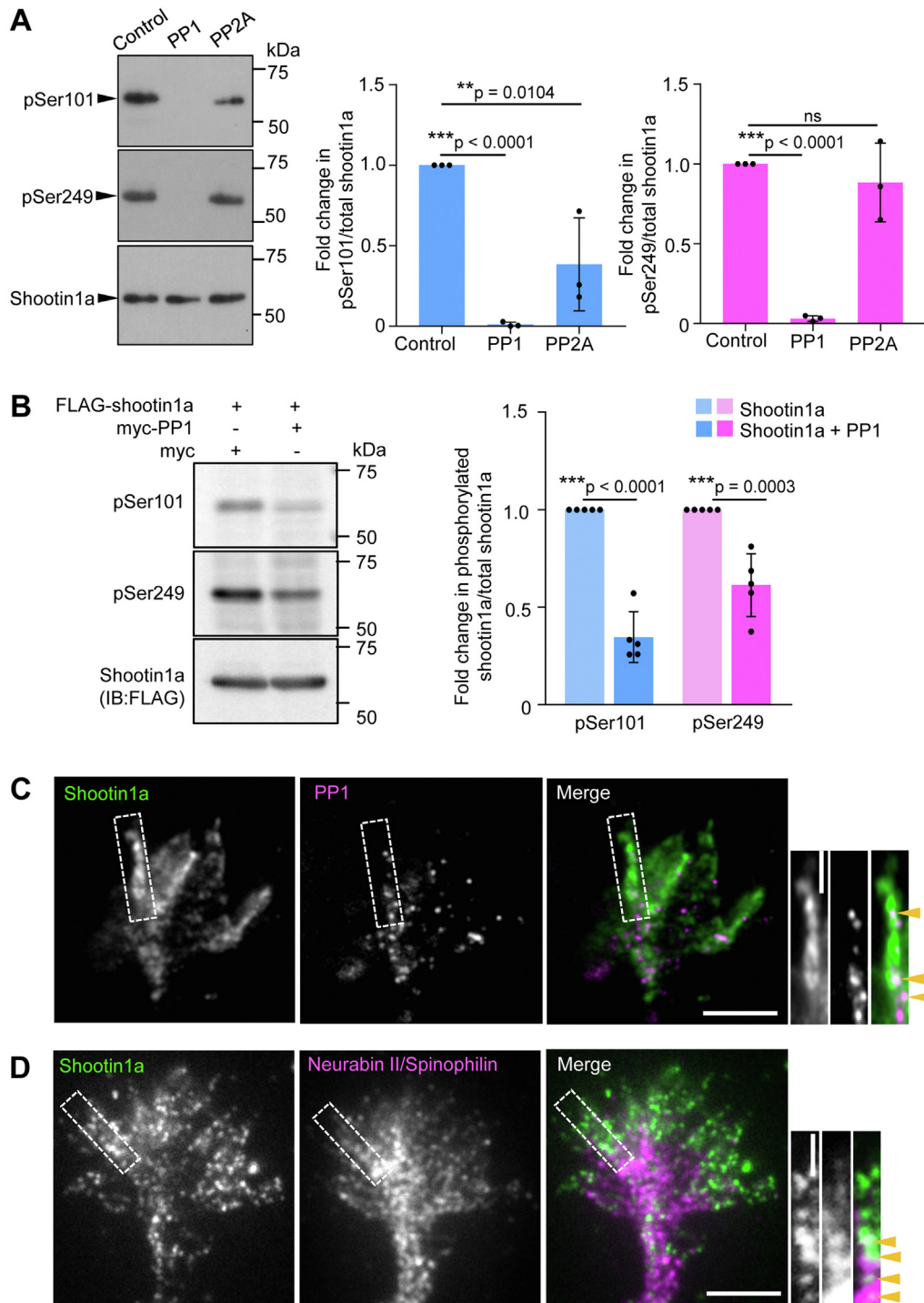
Figure 2. PP1 dephosphorylates shootin1a at Ser101 and Ser249. *A, in vitro* dephosphorylation assays were performed using purified phosphorylated shootin1a. HEK293T cells expressing FLAG-shootin1a were incubated with 200 nM calyculin A for 1 h. Phosphorylated FLAG-shootin1a was then purified by anti-FLAG agarose beads. After a dephosphorylation reaction with PP1 (1.5 mU/μl) or PP2A (1.6 mU/μl), protein mixtures were subjected to SDS-PAGE followed by immunoblot with antibodies against pSer101, pSer249, or shootin1a. The full-length images for immunoblots are presented in Fig. S5*A*. The *right panels* show quantitative analyses of *in vitro* dephosphorylation assays of phosphorylated shootin1a at Ser101 and Ser249 represented as the fold change relative to control (N = 3). *B,* dephosphorylation of shootin1a by PP1 in COS7 cells. Cells were transfected with vectors to express FLAG-shootin1a and myc (control) or with vectors to express FLAG-shootin1a and myc-PP1. Cell lysates were then subjected to SDS-PAGE followed by immunoblotted with antibodies against pSer101, pSer249, or FLAG. The full-length images for immunoblots are presented in Fig. S5*B*. The graphs show quantitative analyses of dephosphorylation assays of shootin1a by PP1 in COS7 cells (N = 5). Fold change of phosphorylated shootin1a was calculated by normalizing by the lysates of control cells. *C,* shootin1a colocalizes with PP1 in axonal growth cones. Fluorescence images of an axonal growth cone (DIV2) of a mouse hippocampal neuron labeled with anti-shootin1a (*green*) and anti-PP1 (*magenta*) antibodies. An enlarged view of the area within the rectangle is shown in the *right panel*. *Arrowheads* indicate shootin1a colocalized with PP1. *D,* shootin1a colocalizes with neurabin-II/spinophilin in axonal growth cones. Fluorescence images of an axonal growth cone (DIV2) of a mouse hippocampal neuron labeled with anti-shootin1a (*green*) and anti-neurabin-II/spinophilin (magenta) antibodies. An enlarged view of the area within the rectangle is shown in the *right panel*. Bar: 5 μm (in the inset: 1 μm). Data represent means ± SD; ***$p < 0.01$; **$p < 0.02$; ns, not significant (One-sample *t* test). DIV, day *in vitro*; PP1, protein phosphatase-1.

shootin1a at both Ser101 and Ser249. On the other hand, PP2A at 1.6 mU/μl partially decreased phosphorylated shootin1a at Ser101, but not at Ser249 (Fig. 2A).

To further analyze the role of PP1 in shootin1a dephosphorylation, PP1 was overexpressed in COS7 cells exogenously expressing shootin1a. Immunoblot analysis showed that overexpressed PP1 significantly reduced the level of phosphorylated shootin1a at both Ser101 and Ser249 (Fig. 2B). Furthermore, immunocytochemical analyses showed that 10 nM tautomycetin increased the fluorescence intensity of phosphorylated shootin1a at Ser249 within growth cones, while overexpression of PP1 reduced it (Fig. S2C). Figure 2C shows the localization of PP1 in the axonal growth cone of a cultured hippocampal neuron. PP1 colocalized partially with shootin1a in growth cones (arrowheads). In addition, shootin1a colocalized with neurabin-II/spinophilin, a cytoskeletal anchoring protein for PP1 (42, 43), in growth cones (arrowheads, Fig. 2D). Although we do not rule out the possibility that other phosphatases may also dephosphorylate shootin1a, these results collectively indicate that PP1 dephosphorylates shootin1a at Ser101 and Ser249 both *in vitro* and in neurons.

PP1 overexpression abolishes netrin-1 gradient–induced asymmetrically localized shootin1a phosphorylation within growth cones

We previously reported that gradients of extracellular netrin-1 elicit asymmetrically localized Pak1-mediated shootin1a phosphorylation within growth cones (11). This in turn promotes asymmetric clutch coupling in growth cones to generate directional forces for growth cone turning toward the netrin-1 source. To analyze the role of PP1-mediated shootin1a dephosphorylation in netrin-1-induced axon guidance, we overexpressed EGFP-PP1 in hippocampal neurons. The PP1 level in neurons transfected with EGFP-PP1 was 3.1 times of that in untransfected neurons (Fig. S2B). To analyze shootin1a phosphorylation within growth cones, neurons overexpressing EGFP (control) or EGFP-PP1 were labeled with the fluorescent volume marker 7-amino-4-chloromethylcoumarin (CMAC), and a netrin-1 gradient was applied approximately perpendicularly to the extending axons for 30 min. They were then fixed and immunolabeled with an antibody that recognizes shootin1a phosphorylation at Ser249 (Fig. 3A). Specificity of the antibody against phosphorylated shootin1a was confirmed by immunolabeling using wildtype and shootin1 knockout neurons: signals of phosphorylated shootin1a were detected in axonal growth cones of wildtype neurons, but not in shootin1 knockout growth cones (Fig. S2A).

As shown in Figure 3A, polarized localization of the phosphorylated shootin1a was observed within control growth cones. The relative level of the phosphorylated shootin1a (phospho-shootin1a immunoreactivity/CMAC staining) was 41% higher on the netrin-1 source side than on the control side (n = 44 growth cones) (Fig. 3B). On the other hand, total shootin1a was detected similarly on the control and netrin-1 source sides (Fig. S3), indicating that the asymmetric localization of pSer249 shootin1a reflects asymmetric phosphorylation rather than asymmetric localization of total shootin1a protein. Overexpression of PP1 abolished the netrin-1-induced asymmetric localization of phospho-shootin1a (n = 49 growth cones) (Fig. 3, A and B).

PP1 overexpression inhibits netrin-1-induced axon turning

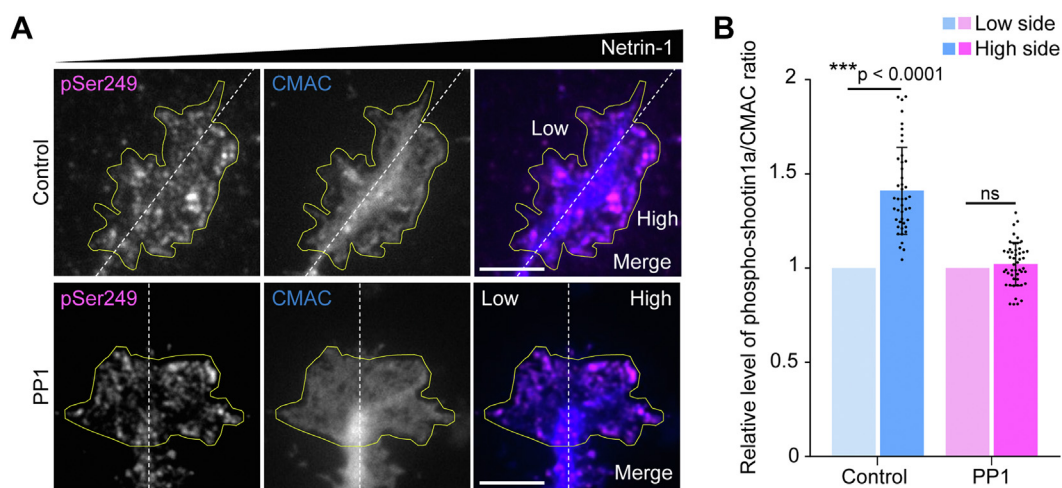Next, we examined whether the disturbance of the asymmetrically localized shootin1a phosphorylation by PP1

Figure 3. PP1 overexpression abolishes netrin-1-induced asymmetric localization of phosphorylated-shootin1a within growth cones. *A*, neurons were transfected with EGFP (control) or EGFP-PP1 (PP1) overexpression plasmid. Transfected neurons cultured for 2 days were labeled with CMAC (*blue*) and exposed to gradients of netrin-1 for 30 min. They were then fixed and immunolabeled with an antibody that recognizes shootin1a phosphorylation at Ser249 (*magenta*). *Solid yellow* and *dashed lines* indicate the boundary and center line of the growth cone, respectively. *B*, quantification of relative phosphorylated shootin1a immunolabeling levels in PP1-overexpressing neurons. After the acquisition of fluorescence images, the growth cone area was divided by the center line (*dotted line*), as the netrin-1 source side (high side) and control side (low side) as shown in *A*. Phospho-shootin1a signals and CMAC signals were quantified in each side to calculate the relative levels of phospho-shootin1a (phospho-shootin1a/CMAC). Then, the ratio (phospho-shootin1a/CMAC) in the high side and low side were compared by normalizing the low side as 1 (N = 3; control, n = 44 growth cones; PP1, n = 49 growth cones). Bars: 5 μm. Data represent means ± SD; ***$p < 0.01$; ns, not significant (One-sample *t* test). CMAC, 7-amino-4-chloromethylcoumarin; PP1, protein phosphatase-1.

overexpression affects axon turning. A netrin-1 gradient was applied approximately perpendicularly to the extending axons of hippocampal neurons overexpressing EGFP (control) or EGFP-PP1. Then, their outgrowth and turning were monitored for 420 min (Fig. 4*A*). The majority of axonal growth cones of control neurons migrated toward the netrin-1 source (Fig. 4*A* and Movie S1). The average axon outgrowth velocity of control neurons was 11.1 ± 1.7 μm/h (Fig. 4*B*), and the net change in the angle of the growth cone toward the netrin-1 source was 47.1 ± 4.0° (n = 22) (Fig. 4*C*). PP1 overexpression not only reduced significantly the axon outgrowth velocity (3.9 ± 0.3 μm/h) (Fig. 4*B*) but also inhibited the growth cone turning toward the netrin-1 source (0.5 ± 8.9°, n = 20) (Fig. 4, *A* and *C* and Movie S2). These results suggest that the disturbance of the asymmetrically localized shootin1a

phosphorylation by PP1 inhibits netrin-1-induced attractive axon guidance.

PP1 inhibition reverses the asymmetrically localized shootin1a phosphorylation within growth cones

To further analyze the role of PP1, we applied tautomycetin to cultured hippocampal neurons. Cultured hippocampal neurons were labeled with the volume marker CMAC, and a netrin-1 gradient was applied to hippocampal neurons in the presence of DMSO (control) or 10 nM tautomycetin for 30 min. They were then fixed and immunolabeled with an antibody that recognizes shootin1a phosphorylation at Ser249. Polarized localization of the phosphorylated shootin1a was observed within control growth cones (Fig. 5*A*). The relative level of the phosphorylated shootin1a (phospho-shootin1a
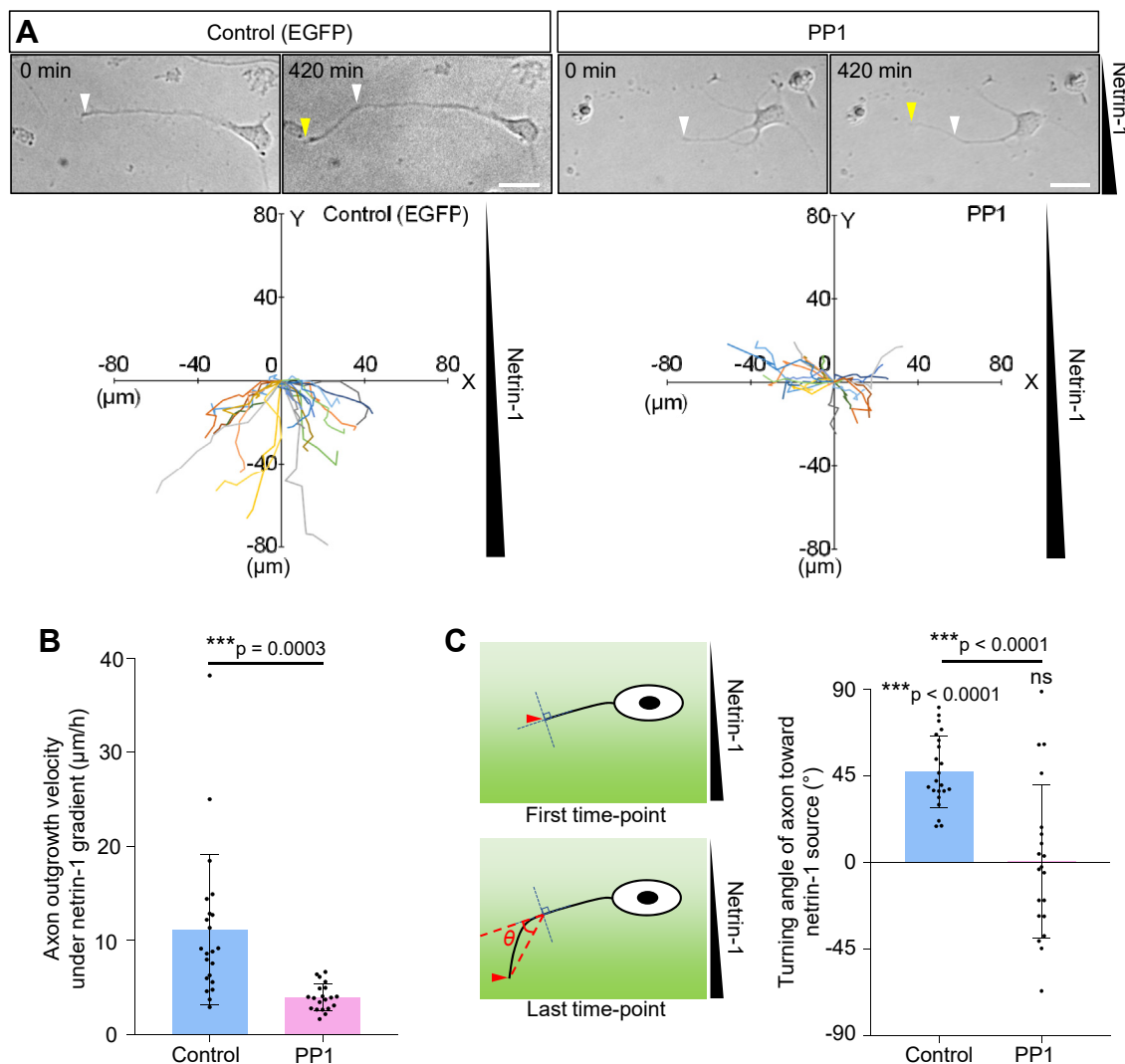

Figure 4. Shootin1a dephosphorylation by PP1 inhibits netrin-1-induced axon guidance. *A*, time-lapse images of hippocampal neurons overexpressing EGFP (control) or EGFP-PP1 under netrin-1 gradients (see Movies S1 and S2). *White* and *yellow arrowheads* indicate growth cones at the first and last timepoints of observation, respectively. The panels below depict trajectories of individual growth cone migrations. The initial growth cone positions are normalized at (X = 0 μm, Y = 0 μm). *B*, axon outgrowth velocity obtained from the analyses in *A* (N = 3; control, n = 22 growth cones; PP1, n = 20 growth cones). *C*, analysis of turning angle under netrin-1 gradients. X and Y axes are set from the growth cone at the first time point. The X axis is drawn along the axonal shaft. Turning angle of axon toward the netrin-1 source was measured from control and PP1-overexpressing neurons. The graph shows quantified data (N = 3; control, n = 22 growth cones; PP1, n = 20 growth cones). Bars: 20 μm. Data represent means ± SD; ***p < 0.01 (*B*, unpaired Student's *t* test; *C*, unpaired and paired Student's *t* test). PP1, protein phosphatase-1.
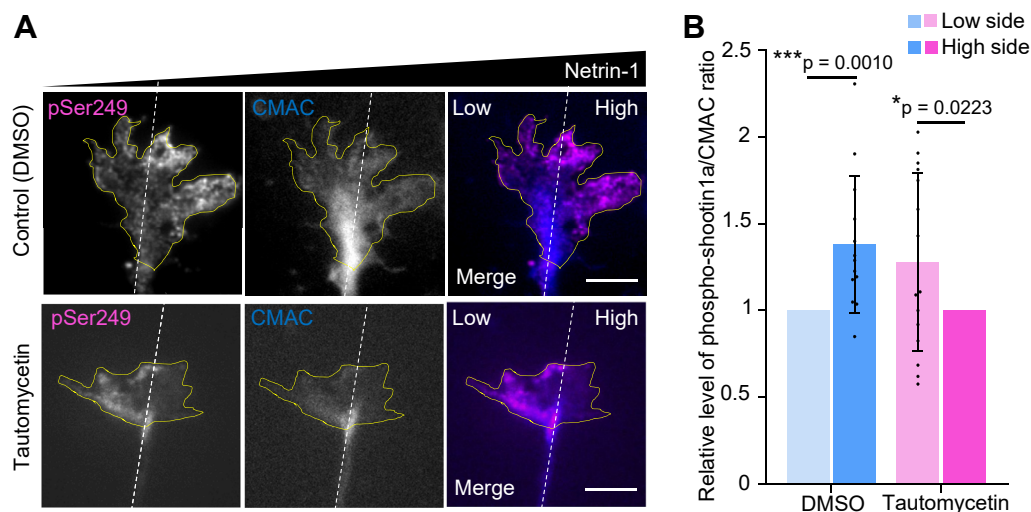
Figure 5. PP1 inhibition reverses netrin-1-induced asymmetric localization of phosphorylated shootin1a within growth cones. *A*, hippocampal neurons (DIV2) were labeled with the volume marker CMAC (*blue*). Neurons were pretreated with DMSO (control) or 10 nM tautomycetin for 30 min and exposed to gradients of netrin-1 for 30 min. They were then fixed and immunolabeled with an antibody that recognizes shootin1a phosphorylation at Ser249 (*magenta*). *Solid yellow lines* indicate the boundary of the growth cone. *B*, quantification of relative phospho-shootin1a levels in control and tautomycetin-treated neurons. After the acquisition of fluorescence images, the growth cone area was divided by the center line (*dotted line*), as the netrin-1 source side (high side) and control side (low side) as shown in *A*. Phospho-shootin1a signals and CMAC signals were quantified in each side to calculate the relative levels of phospho-shootin1a (phospho-shootin1a/CMAC). Then, the ratio (phospho-shootin1a/CMAC) in the high side and low side were compared by normalizing the low side was as one in the control (DMSO) growth cones. In the tautomycetin-treated growth cones, the ratio in the high side was normalized as 1 (N = 3; control, n = 13 growth cones; tautomycetin, n = 15 growth cones). Bars: 5 μm. Data represent means ± SD; ***$p < 0.01$; *$p < 0.05$; ns, not significant (One-sample *t* test). CMAC, 7-amino-4-chloromethylcoumarin; DIV, day *in vitro*; PP1, protein phosphatase-1.

immunoreactivity/CMAC staining) was 38% higher on the netrin-1 source side than on the control side (n = 13 growth cones) (Fig. 5*B*). Remarkably, inhibition of PP1 by tautomycetin reversed the asymmetrically localized shootin1a phosphorylation under netrin-1 (Fig. 5*A*): the phosphorylated shootin1a was 28% higher on the control side than on the netrin-1 source side (n = 15 growth cones) (Fig. 5*B*).

PP1 inhibition changes the netrin-1-induced growth cone turning from attraction to repulsion

Finally, we examined whether the reversal of the asymmetrically localized shootin1a phosphorylation by PP1 inhibition affects axon turning. To address this question, a netrin-1 gradient was applied to the extending axons of hippocampal neurons in presence of DMSO (control) or 10 nM tautomycetin. Their outgrowth and turning were then monitored for 420 min. In the absence of tautomycetin, a majority of axonal growth cones migrated toward the netrin-1 source (Fig. 6*A* and Movie S3). The average axon outgrowth velocity of control neurons was 19.2 ± 2.4 μm/h (Fig. 6*B*), and the net change in the angle of the growth cone toward the netrin-1 source was 42.6 ± 4.8° (n = 21 growth cones) (Fig. 6*C*). PP1 inhibition by tautomycetin decreased the axon outgrowth velocity (13.4 ± 1.1 μm/h) (Fig. 6*B*). Furthermore, in the presence of tautomycetin, a majority of axonal growth cones showed repulsive responses (Fig. 6*A* and Movie S4): the net change in the angle of the growth cone toward the netrin-1 source was −29.6 ± 7.2° (n = 23 growth cones) (Fig. 6*C*). These results suggest that reversal of the asymmetrically localized shootin1a phosphorylation by PP1 inhibition changes netrin-1-induced growth cone turning from attraction to repulsion.

Discussion

PP1 dephosphorylates shootin1a for netrin-1-induced axon guidance

Previous studies reported that stimulation of hippocampal neurons by netrin-1 elicits Pak1-mediated shootin1a phosphorylation at Ser101 and Ser249 (red arrows, Fig. 7*A*) (11, 23). The phosphorylation at these sites enhances shootin1a–cortactin and shootin1a–L1-CAM interactions in growth cones, thereby promoting of the traction force (pink arrows) for growth cone migration (white arrows) (11, 26). The present study demonstrates that PP1 dephosphorylates shootin1a at these sites (blue arrow).

Gradients of extracellular netrin-1 concentration induce asymmetrically localized shootin1a phosphorylation within growth cones, which is higher on the netrin-1 source side. This in turn promotes shootin1a-mediated local actin–adhesion coupling within growth cones, generating directional forces for growth cone turning toward the netrin-1 source (white arrow, Fig. 7*A*) (11). In addition, replacement of wildtype shootin1a with a phospho-mimic shootin1a mutant, which cannot be activated in the asymmetric manner by phosphorylation, abolishes growth cone turning toward the netrin-1 source (11). Here, PP1 overexpression abolished the netrin-1-induced asymmetric localization of phosphorylated-shootin1a as well as axon turning. Furthermore, inhibition of PP1 activity by tautomycetin reversed the asymmetrically localized shootin1a phosphorylation, thereby changing the netrin-1-induced growth cone turning from attraction to repulsion. Collectively, these data support the notion that asymmetric shootin1a phosphorylation within growth cones mediates netrin-1-induced axon turning (Fig. 7*A*). In addition,
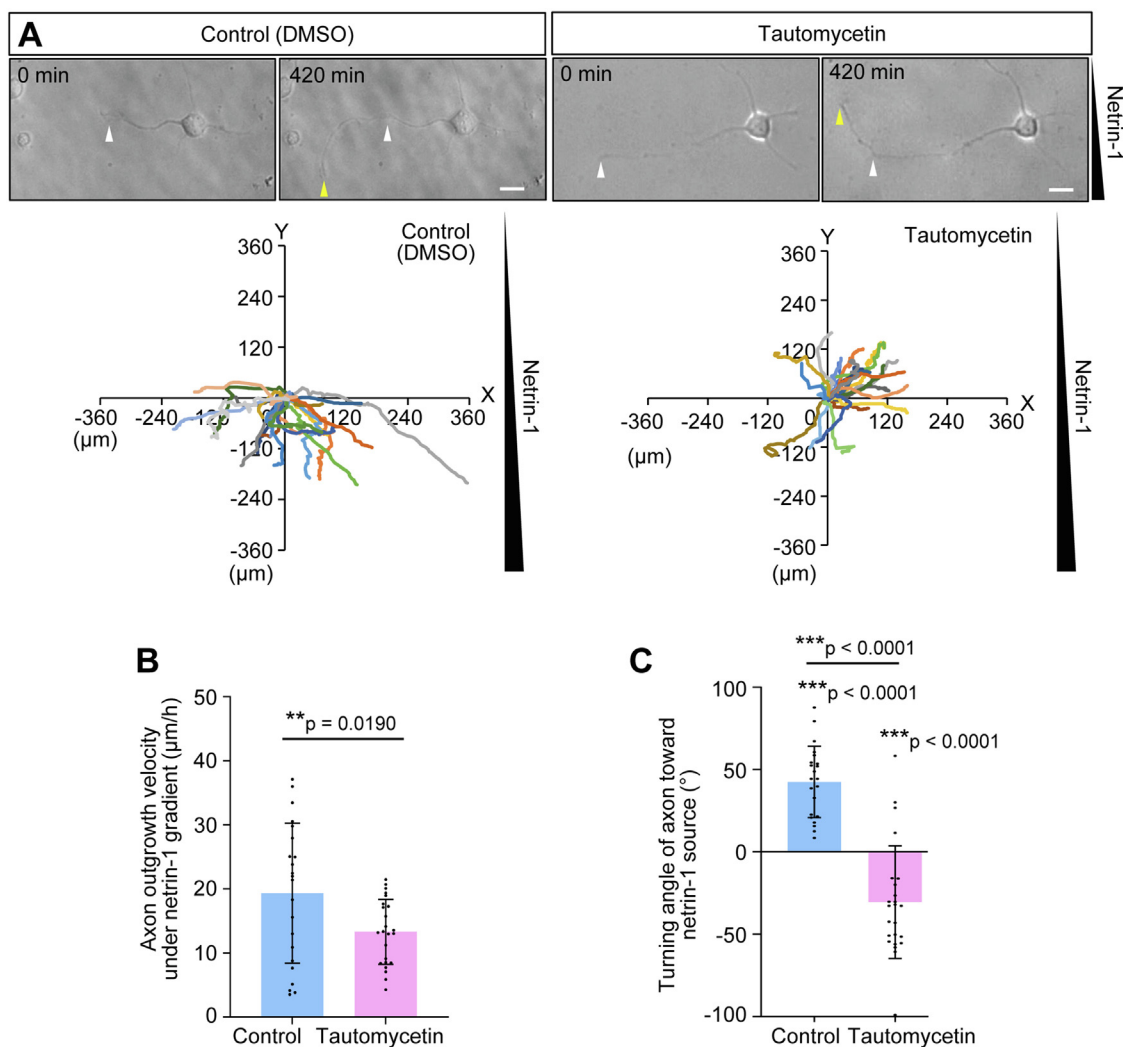
Figure 6. PP1 inhibition changes the netrin-1-induced growth cone turning from attraction to repulsion. *A*, time-lapse images of axonal growth cone migration under netrin-1 gradients. Hippocampal neurons were pretreated with DMSO (control) or 10 nM tautomycetin before the gradients were generated (see Movies S3 and S4). *White* and *yellow arrowheads* indicate growth cones at the first and last timepoints of observation, respectively. The panels below depict trajectories of individual growth cone migrations. The initial growth cone positions are normalized at (X = 0 µm, Y = 0 µm). *B*, axon outgrowth velocity obtained from the analyses in *A* (N = 3; control, n = 22 growth cones; tautomycetin, n = 24 growth cones). *C*, turning angles (θ) were obtained from analyses in *A*, by calculating the difference between the angles of the axonal tip at the first and last timepoints of the observations (*red arrowheads*). The graph shows quantified data (N = 3; control, n = 22 growth cones; tautomycetin, n = 24 growth cones). Bars: 20 µm. Data represent means ± SD; ***$p < 0.01$; **$p < 0.02$; ns, not significant (*B*, unpaired Student's *t* test; *C*, unpaired and paired Student's *t* test). PP1, protein phosphatase-1.

the present findings suggest that PP1-mediated turnover of phosphorylated shootin1 is required for proper axon guidance induced by netrin-1.

Possible desensitization of the netrin-1–Pak1–shootin1a pathway for long-distance chemotaxis

It is unclear how PP1 inhibition reverses the asymmetrically localized shootin1a phosphorylation. However, we consider that this reversal may result from a local desensitization of the netrin-1–Pak1–shootin1a signaling pathway (Fig. 7B). Taylor *et al.* (44) reported that increasing the basal netrin-1 concentration reverses the growth cone turning of mouse cortical axons under netrin-1 gradients from attraction to repulsion. Our data are consistent with this report, as both PP1 inhibition and an increase in netrin-1 concentration upregulate the basal level of phospho-shootin1a (Fig. 7A).

Ming *et al.* (45) reported that *Xenopus* spinal neurons exhibit a zig-zag pattern of growth cone migration toward a micropipette providing netrin-1, through repeated chemoattraction and repulsion (45). As bath application of netrin-1 at high concentration desensitizes the attractive growth cone response, they proposed that local desensitization of netrin-1 signaling within growth cone may occur during the zig-zag chemotaxis. If a local excess of the netrin-1–Pak1–shootin1a signaling desensitizes itself, the signal which exceeds a threshold through PP1 inhibition could locally desensitize it at the netrin source side, thereby reducing the phosphorylated shootin1a at this side and inducing the repulsive response (Fig. 7B).

For long-distance chemotaxis, growth cones not only sense subtle spatial differences in chemical cues for their turning but also have to adjust their sensitivity repeatedly in order to migrate through various environments where the basal
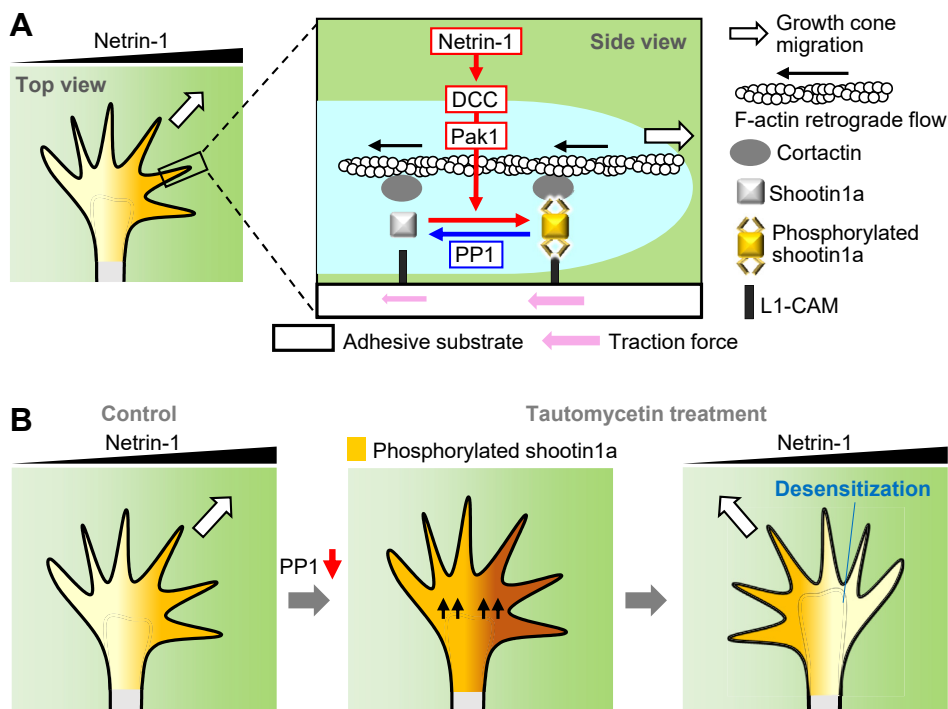
Figure 7. A model for the involvement of PP1 in netrin-1-induced axon guidance. *A*, gradients of extracellular netrin-1 concentration induce asymmetrically localized shootin1a phosphorylation at Ser101 and Ser249 within growth cones, which is higher on the netrin-1 source side. The phosphorylation at these sites enhances shootin1a–cortactin and shootin1a–L1-CAM interactions in growth cones, thereby promoting the traction force (*pink arrows*) for growth cone migration (*white arrow*). On the other hand, PP1 dephosphorylates shootin1a at these sites (*blue arrow*). Shootin1a dephosphorylation by PP1 plays a key role in organizing asymmetrically localized phospho-shootin1a within growth cones, which is required for netrin-1-induced attractive axon guidance. *B*, a possible explanation for how PP1 inhibition reverses the asymmetrically localized shootin1a phosphorylation under netrin-1 gradient. PP1 inhibition by tautomycetin increases basal levels of phosphorylated shootin1a (*middle panel*). A local excess of the netrin-1–Pak1–shootin1a signaling desensitize itself at the netrin source side, thereby reducing the phosphorylated shootin1a at this side and inducing the repulsive response (*right panel*). DCC, deleted in colorectal cancer; PP1, protein phosphatase-1.

concentration of a chemical cue changes substantially. Desensitization and re-adaptation are thought to adjust the sensitivity to broad-range concentrations of chemoattractants during long-distance migration (45, 46). PP1 might be involved in the adjustment of growth cone sensitivity to chemoattractants for proper navigation.

PP1 in shootin1-mediated neural wiring processes

Recent studies reported that Pak1-mediated shootin1a phosphorylation also regulates structural plasticity of dendritic spines (47) and actin wave propagation which is required for axonal extension (48, 49). In relation to these reports, PP1 mediates synaptic signaling and plasticity (36, 50–52). On the other hand, shootin1b, a splicing variant of shootin1a that contains the phosphorylation sites Ser101 and Ser249 (53), was reported to mediate neuronal migration (54). These findings raise the possibility that PP1-mediated shootin1a dephosphorylation may be involved in the regulation of multiple steps in neural wiring processes.

In conclusion, the present study identified PP1 as a protein phosphatase that dephosphorylates shootin1a. At present, it remains a mystery how PP1 inhibition reverses the asymmetrically localized phospho-shootin1a. In addition, it is unclear how PP1 and Pak1 contribute to the transduction of subtle spatial differences in extracellular netrin-1 concentration into the asymmetrically localized phospho-shootin1a within growth cones. Future detailed analyses of the signaling networks involving PP1 and Pak1 will lead to a better understanding of the exquisitely sensitive chemosensory and motile behaviors of growth cones.

Experimental procedures

Cultures and transfection

All relevant aspects of the experimental procedures were approved by the Institutional Animal Care and Use Committee of Nara Institute of Science and Technology (reference no. 1802). Cortical and hippocampal neurons were prepared from embryonic day 16.5 mouse embryos. Hippocampal neurons were cultured on glass coverslips coated successively with poly-D-lysine (Sigma, catalog number: P-6407) and L1-CAM-Fc as described previously (11, 25). For immunoblot analyses in Figure 1, we used cortical neurons as the experiments required large numbers of neurons; they were cultured on poly-D-lysine–coated dishes. The neurons were transfected with vectors using Nucleofector (Lonza) before plating. HEK293T (ATCC, CVCL_0063) and COS7 (RIKEN BRC, RBRC-RCB0539) cells were cultured in Dulbecco's modified Eagle's medium (Sigma, catalog number: D6429) supplemented with 10% fetal bovine serum and transfected with plasmid DNA using Polyethylenimine MAX (PEI MAX,

Polysciences, catalog number: 24765) following the manufacturer's protocol.

DNA constructs

Preparation of vectors to express shootin1a has been described previously (55). cDNA of PP1 catalytic subunit alpha was amplified from mouse brain cDNA by PCR with the primers 5′-ATAGGATCCATGTCCGACAGCGAGAAGCT-3′ and 5′-GCGAGTCGACCTATTTCTTGGCTTTGGCG-GAATTGC-3′ and then subcloned into pCMV-myc and pCAGGS-EGFP vectors.

Immunoblot

Immunoblot was performed as described (10, 11). For determining phosphorylated shootin1a in the presence of phosphatase inhibitors, DIV3 cortical neurons (2×10^6 cells) were incubated for 1 h with the following inhibitors: 200 nM calyculin A (Santa Cruz Biotechnology, catalog number: sc-24000), 100 nM okadaic acid (Sigma, catalog number: o9381), 10 nM Fostriecin (Tocris, catalog number: 1840), 50 nM FK506 (Tocris, catalog number: 3631), and 10 nM tautomycetin (Tocris, catalog number: 2305). Cell lysates were collected using RIPA buffer (50 mM Tris-HCl pH 8.0, 150 mM NaCl, 1 mM EDTA, 1% Triton X-100, 0.1% SDS, 0.1% sodium deoxycholate, 1 mM DTT, 1 mM PMSF, 0.01 mM leupeptin). Immunoblot was performed using rabbit anti-pSer101-shootin1 antibody (23) at 1:1000 dilution or rabbit anti-pSer249-shootin1 antibody (23) at 1:5000 dilution, rabbit shootin1a antibody (11) at 1:5000 dilution as described (10, 11), and rabbit anti-phospho histone H3 (Ser10) (Millipore, catalog number: 06-570) at 1:1000 dilution. For dephosphorylation assay of shootin1a in cells, COS7 cells were transfected with pCMV-FLAG-shootin1a together with pCMV-myc (control) or pCMV-myc-PP1 using PEI MAX. Transfected COS7 cell lysates were then collected using RIPA buffer at 48 h posttransfection. Immunoblot was performed using rabbit anti-FLAG antibody (MBL, catalog number: PM020) at 1:1000 dilution and rabbit anti-myc antibody (MBL, catalog number: 562-5) at 1:2000 dilution as described (10, 11).

Immunocytochemistry and microscopy

Cultured neurons were fixed with 3.7% formaldehyde (Nacalai Tesque, catalog number: 16223-55) dissolved in Krebs buffer (118 mM NaCl, 5.7 mM KCl, 1.2 mM KH$_2$PO$_4$, 1.2 mM MgSO$_4$, 4.2 mM NaHCO$_3$, 2 mM CaCl$_2$, 10 mM glucose, 400 mM sucrose, 10 mM Hepes pH 7.2) for 10 min at room temperature, followed by treatment with 0.05% Triton X-100 in PBS for 15 min on ice and 10% fetal bovine serum in PBS for 1 h at room temperature. They were then incubated with primary antibodies diluted in PBS containing 10% fetal bovine serum overnight at 4 °C. The following primary antibodies were used: rabbit anti-pSer249-shootin1 antibody at 1:2000 dilution, rabbit anti-shootin1a antibody at 1:2000 dilution, mouse anti-PP1 antibody (Santa Cruz Biotechnology, catalog number: sc-7482) at 1:500 dilution, rabbit anti-Myc

antibody (MBL, catalog number: 562-5) at 1:500 dilution, rabbit anti-neurabin-II/spinophilin antibody (Sigma, catalog number: N5037) at 1:500 dilution, and mouse anti-GFP antibody (MBL, catalog number: M048-3) at 1:2000 dilution. Neurons were washed with PBS, and then incubated with secondary antibodies diluted in PBS for 1 h at room temperature. The following secondary antibodies were used: Alexa Fluor 594-conjugated donkey anti-rabbit (Jackson ImmunoResearch Laboratories, catalog number: 711-585-152) at 1:1000 dilution, Alexa Fluor 488-conjugated goat anti-rabbit (Invitrogen, catalog number: A-11008) at 1:1000 dilution, and Alexa Fluor 594-conjugated goat anti-mouse (Invitrogen, catalog number: A-11032) at 1:1000 dilution. For phalloidin staining, after washing with PBS, cells were stained with Alexa Fluor 594-conjugated phalloidin (Invitrogen, catalog number: A12381) at 1:100 dilution for 30 min at room temperature. Immunostained cells were mounted with 50% (v/v) glycerol in PBS.

Fluorescence images were acquired using a fluorescence microscope (Axioplan2; Carl Zeiss) equipped with a plan-Apochromat 100 × 1.40 oil objective (Carl Zeiss), a charge-coupled device camera (AxioCam MRm, Carl Zeiss), and imaging software (Axiovision3, Carl Zeiss). Live-cell images of cultured hippocampal neurons were acquired at 37 °C using a fluorescence microscope (IX81; Olympus) equipped with an EM-charge-coupled device camera (Ixon3; Andor), a CMOS camera (ORCA Flash4.0LT; Hamamatsu), an UplanApo 20 × 0.7 NA (Olympus), and imaging software (MetaMorph, Molecular Devices). Axon outgrowth, trajectories, and turning were measured using ImageJ (Fiji version).

For quantification of the antibody signals in growth cones in Figures 3A and 5A, we labeled neurons with the fluorescent volume marker CMAC to avoid an influence of the difference in the growth-cone thickness. For CMAC staining, neurons were incubated with 2.5 μM CMAC (Invitrogen, catalog number: C2110) for 1 h before generation of netrin-1 gradients. After the acquisition of fluorescence images, the growth cone area was divided by the center line extended from the axonal shaft (dotted line, Figs. 3A and 5A), as the netrin-1 source side (high side) and control side (low side). Phospho-shootin1a signals and CMAC signals were quantified in each side to calculate the relative level of phospho-shootin1a (phospho-shootin1a/CMAC). Then, the ratio (phospho-shootin1a/CMAC) in the high side and low side were compared by normalizing the low side as 1 in the control/ DMSO and PP1 expressing growth cones (Figs. 3B and 5B). On the other hand, in the tautomycetin-treated growth cones the ratio (phospho-shootin1a/CMAC) in the high side was normalized as 1 (Fig. 5B).

Protein preparation and *in vitro* phosphatase assay

FLAG-shootin1a was expressed in HEK293T cells. To increase phosphorylated FLAG-shootin1a in HEK293T cells, the cells were treated with calyculin A (200 nM) for 1 h. Phosphorylated FLAG-shootin1a was then purified using anti-FLAG M2 gels (Sigma, catalog number: A2220). Recombinant

human PP1 alpha and bovine PP2A$_2$ were purchased from Novus Biologicals (catalog number: NBP1-72418) and Sigma (product number: P1868), respectively. Phosphatase reactions were carried out in PP1 reaction buffer (10 mM Tris-HCl pH 7.0, 50 mM NaCl, 2 mM DTT, 1 mM MnCl$_2$) or PP2A reaction buffer (50 mM Tris-HCl pH 7.0, 150 mM NaCl, 1 mM DTT, 1 mM MnCl$_2$) containing 1.5 mU/μl PP1 or 1.6 mU/μl PP2A and 15 ng phosphorylated FLAG-shootin1a. As PP1 at 1.5 mU/μl and PP2 at 1.6 mU/μl dephosphorylated an equivalent amount of the nonpeptide substrate DiFMUP (56) (Tocris Bioscience, catalog number: 6882) (Fig. S6), the enzymes at these concentrations were used in the shootin1a dephosphorylation assay. The reactions were performed at 30 °C for 3 h. Immunoblot of phosphorylated shootin1a was then performed.

Axon guidance assay

A microfluidic device to generate netrin-1 gradients in culture medium was produced according to previous reports (10, 11). Briefly, the microfluidic device was fabricated with polydimethylsiloxane (PDMS; Silpot 184, Dow Corning Toray, catalog number: 3255981) and attached to a glass coverslip. The device consists of a cell culture area and two microchannels along the two sides of the culture area. The micromolds of the channel pattern were lithographically fabricated on a photoresist (SU-8 3025, MicroChem) spin-coated on a 70-μm thick silicon wafer. PDMS sheets were fabricated from the mold, which had been coated with silicone oil (Barrier coat No. 6, ShinEtsu, catalog number: 06003) to facilitate their removal. A PDMS sheet was then bonded to a glass coverslip using plasma irradiation (Sakigake, catalog number: YHS-R). The glass coverslip was coated with poly-D-lysine and L1-CAM-Fc.

For guidance assays under PP1 inhibition, cultured neurons were pretreated with DMSO (control) or 10 nM tautomycetin for 30 min before netrin-1 gradient generation; guidance assays were performed in the presence of DMSO or 10 nM tautomycetin. For live imaging of neurons overexpressing EGFP-PP1, EGFP fluorescence was used as an indicator of PP1 overexpression. Neurons at DIV1.5 to 2 were used for time-lapse imaging. To generate netrin-1 gradients in the cell culture area, flows of culture medium with or without 300 ng/ml netrin-1 (R&D Systems, catalog number: 1109-N1-025) were applied to the microchannels on either side of the cell culture area for 420 min.

For analysis of turning angle under netrin-1 gradients, X and Y axes were set from the growth cone at the first timepoint. The X axis was drawn along the axon shaft. Turning angles (θ) were obtained by calculating the difference between the angles of the axonal tip at the first and last timepoints of the observations (Fig. 4*C*).

Statistical analyses

All statistical analyses were performed using Microsoft Excel and GraphPad Prism7 (GraphPad Software).

Significance was determined by the one-sample *t* test, two-tailed Student's *t* test, and one-way ANOVA with Tukey`s multiple comparison test. For the analyses of attraction or repulsion axon turning, we used the paired *t* test comparing turning angles between the first (zero degree) and last timepoints.

Data availability

All data are contained within this article. Reagents and plasmids described in this article are available upon request.

Conflict of interest—The authors declare no conflicts of interest with the contents of this article.

Abbreviations—The abbreviations used are: CMAC, 7-amino-4-chloromethylcoumarin; DIV, day *in vitro*; F-actin, actin filament; PDMS, polydimethylsiloxane; PP1, protein phosphatase-1.

References

1. Dent, E. W., and Gertler, F. B. (2003) Cytoskeletal dynamics and transport in growth cone motility and axon guidance. *Neuron* **40**, 209–227
2. Lowery, L. A., and Van Vactor, D. (2009) The trip of the tip: understanding the growth cone machinery. *Nat. Rev. Mol. Cell Biol.* **10**, 332–343
3. Vitriol, E. A., and Zheng, J. Q. (2012) Growth cone travel in space and time: the cellular ensemble of cytoskeleton, adhesion, and membrane. *Neuron* **73**, 1068–1081
4. Gomez, T. M., and Letourneau, P. C. (2014) Actin dynamics in growth cone motility and navigation. *J. Neurochem.* **129**, 221–234
5. Rosoff, W. J., Urbach, J. S., Esrick, M. A., McAllister, R. G., Richards, L. J., and Goodhill, G. J. (2004) A new chemotaxis assay shows the extreme sensitivity of axons to molecular gradients. *Nat. Neurosci.* **7**, 678–682
6. Xiao, R. R., Wang, L., Zhang, L., Liu, Y. N., Yu, X. L., and Huang, W. H. (2014) Quantifying biased response of axon to chemical gradient steepness in a microfluidic device. *Anal. Chem.* **86**, 11649–11656
7. Miller, K. E., and Suter, D. M. (2018) An integrated cytoskeletal model of neurite outgrowth. *Front. Cell Neurosci.* **12**, 447
8. McCormick, L. E., and Gupton, S. L. (2020) Mechanistic advances in axon pathfinding. *Curr. Opin. Cell Biol.* **63**, 11–19

9. Franze, K. (2020) Integrating chemistry and mechanics: the forces driving axon growth. *Annu. Rev. Cell Dev. Biol.* **36**, 61–83

10. Abe, K., Katsuno, H., Toriyama, M., Baba, K., Mori, T., Hakoshima, T., *et al.* (2018) Grip and slip of L1-CAM on adhesive substrates direct growth cone haptotaxis. *Proc. Natl. Acad. Sci. U. S. A.* **115**, 2764–2769

11. Baba, K., Yoshida, W., Toriyama, M., Shimada, T., Manning, C. F., Saito, M., *et al.* (2018) Gradient-reading and mechano-effector machinery for netrin-1-induced axon guidance. *Elife* **7**, e34593

12. Ishii, N., Wadsworth, W. G., Stern, B. D., Culotti, J. G., and Hedgecock, E. M. (1992) UNC-6, a laminin-related protein, guides cell and pioneer axon migrations in C. elegans. *Neuron* **9**, 873–881

13. Serafini, T., Kennedy, T. E., Galko, M. J., Mirzayan, C., Jessell, T. M., and Tessier-Lavigne, M. (1994) The netrins define a family of axon outgrowth-promoting proteins homologous to C. elegans UNC-6. *Cell* **78**, 409–424

14. Lai Wing Sun, K., Correia, J. P., and Kennedy, T. E. (2011) Netrins: versatile extracellular cues with diverse functions. *Development* **138**, 2153–2169

15. Kennedy, T. E., Serafini, T., de la Torre, J. R., and Tessier-Lavigne, M. (1994) Netrins are diffusible chemotropic factors for commissural axons in the embryonic spinal cord. *Cell* **78**, 425–435

16. Fazeli, A., Dickinson, S. L., Hermiston, M. L., Tighe, R. V., Steen, R. G., Small, C. G., *et al.* (1997) Phenotype of mice lacking functional deleted in colorectal cancer (Dcc) gene. *Nature* **386**, 796–804

17. Bin, J. M., Han, D., Lai Wing Sun, K., Croteau, L. P., Dumontier, E., Cloutier, J. F., *et al.* (2015) Complete loss of netrin-1 results in embryonic lethality and severe axon guidance defects without increased neural cell death. *Cell Rep.* **12**, 1099–1106

18. Wu, Z., Makihara, S., Yam, P. T., Teo, S., Renier, N., Balekoglu, N., *et al.* (2019) Long-range guidance of spinal commissural axons by netrin1 and sonic hedgehog from midline floor plate cells. *Neuron* **101**, 635–647

19. Forscher, P., and Smith, S. J. (1988) Actions of cytochalasins on the organization of actin filaments and microtubules in a neuronal growth cone. *J. Cell Biol.* **107**, 1505–1516

20. Katoh, K., Hammar, K., Smith, P. J., and Oldenbourg, R. (1999) Birefringence imaging directly reveals architectural dynamics of filamentous actin in living growth cones. *Mol. Biol. Cell* **10**, 197–210

21. Mitchison, T., and Kirschner, M. (1988) Cytoskeletal dynamics and nerve growth. *Neuron* **1**, 761–772

22. Suter, D. M., and Forscher, P. (2000) Substrate-cytoskeletal coupling as a mechanism for the regulation of growth cone motility and guidance. *J. Neurobiol.* **44**, 97–113

23. Toriyama, M., Kozawa, S., Sakumura, Y., and Inagaki, N. (2013) Conversion of a signal into forces for axon outgrowth through Pak1-mediated shootin1 phosphorylation. *Curr. Biol.* **23**, 529–534

24. Mogilner, A., and Oster, G. (1996) Cell motility driven by actin polymerization. *Biophys. J.* **71**, 3030–3045

25. Shimada, T., Toriyama, M., Uemura, K., Kamiguchi, H., Sugiura, T., Watanabe, N., *et al.* (2008) Shootin1 interacts with actin retrograde flow and L1-CAM to promote axon outgrowth. *J. Cell Biol.* **181**, 817–829

26. Kubo, Y., Baba, K., Toriyama, M., Minegishi, T., Sugiura, T., Kozawa, S., *et al.* (2015) Shootin1-cortactin interaction mediates signal-force transduction for axon outgrowth. *J. Cell Biol.* **210**, 663–676

27. Li, X., Saint-Cyr-Proulx, E., Aktories, K., and Lamarche-Vane, N. (2002) Rac1 and Cdc42 but not RhoA or Rho kinase activities are required for neurite outgrowth induced by the Netrin-1 receptor DCC (deleted in colorectal cancer) in N1E-115 neuroblastoma cells. *J. Biol. Chem.* **277**, 15207–15214

28. Shekarabi, M., and Kennedy, T. E. (2002) The netrin-1 receptor DCC promotes filopodia formation and cell spreading by activating Cdc42 and Rac1. *Mol. Cell. Neurosci.* **19**, 1–17

29. Shekarabi, M., Moore, S. W., Tritsch, N. X., Morris, S. J., Bouchard, J. F., and Kennedy, T. E. (2005) Deleted in colorectal cancer binding netrin-1 mediates cell substrate adhesion and recruits Cdc42, Rac1, Pak1, and N-WASP into an intracellular signaling complex that promotes growth cone expansion. *J. Neurosci.* **25**, 3132–3141

30. Briancon-Marjollet, A., Ghogha, A., Nawabi, H., Triki, I., Auziol, C., Fromont, S., *et al.* (2008) Trio mediates netrin-1-induced Rac1 activation in axon outgrowth and guidance. *Mol. Cell. Biol.* **28**, 2314–2323

31. Demarco, R. S., Struckhoff, E. C., and Lundquist, E. A. (2012) The Rac GTP exchange factor TIAM-1 acts with CDC-42 and the guidance receptor UNC-40/DCC in neuronal protrusion and axon guidance. *PLoS Genet.* **8**, e1002665

32. Cohen, P. (1989) The structure and regulation of protein phosphatases. *Annu. Rev. Biochem.* **58**, 453–508

33. Cohen, P. T. W. (2002) Protein phosphatase 1 - targeted in many directions. *J. Cell Sci.* **115**, 241–256

34. Shi, Y. (2009) Serine/threonine phosphatases: mechanism through structure. *Cell* **139**, 468–484

35. Inagaki, N., Ito, M., Nakano, T., and Inagaki, M. (1994) Spatiotemporal distribution of protein kinase and phosphatase activities. *Trends Biochem. Sci.* **19**, 448–452

36. Colbran, R. J. (2004) Protein phosphatases and calcium/calmodulin-dependent protein kinase II-dependent synaptic plasticity. *J. Neurosci.* **24**, 8404–8409

37. Wen, Z., Guirland, C., Ming, G. L., and Zheng, J. Q. (2004) A CaMKII/calcineurin switch controls the direction of Ca(2+)-dependent growth cone guidance. *Neuron* **43**, 835–846

38. Hoffman, A., Taleski, G., and Sontag, E. (2017) The protein serine/threonine phosphatases PP2A, PP1 and calcineurin: a triple threat in the regulation of the neuronal cytoskeleton. *Mol. Cell. Neurosci.* **84**, 119–131

39. Pribiag, H., and Stellwagen, D. (2013) TNF-alpha downregulates inhibitory neurotransmission through protein phosphatase 1-dependent trafficking of GABA(A) receptors. *J. Neurosci.* **33**, 15879–15893

40. Choy, M. S., Swingle, M., D'Arcy, B., Abney, K., Rusin, S. F., Kettenbach, A. N., *et al.* (2017) PP1:tautomycetin complex reveals a path toward the development of PP1-specific inhibitors. *J. Am. Chem. Soc.* **139**, 17703–17706

41. Engmann, O., Giralt, A., Gervasi, N., Marion-Poll, L., Gasmi, L., Filhol, O., *et al.* (2015) DARPP-32 interaction with adducin may mediate rapid environmental effects on striatal neurons. *Nat. Commun.* **6**, 10099

42. Allen, P. B., Ouimet, C. C., and Greengard, P. (1997) Spinophilin, a novel protein phosphatase 1 binding protein localized to dendritic spines. *Proc. Natl. Acad. Sci. U. S. A.* **94**, 9956–9961

43. Bielas, S. L., Serneo, F. F., Chechlacz, M., Deerinck, T. J., Perkins, G. A., Allen, P. B., *et al.* (2007) Spinophilin facilitates dephosphorylation of doublecortin by PP1 to mediate microtubule bundling at the axonal wrist. *Cell* **129**, 579–591

44. Taylor, A. M., Menon, S., and Gupton, S. L. (2015) Passive microfluidic chamber for long-term imaging of axon guidance in response to soluble gradients. *Lab. Chip* **15**, 2781–2789

45. Ming, G. L., Wong, S. T., Henley, J., Yuan, X. B., Song, H. J., Spitzer, N. C., *et al.* (2002) Adaptation in the chemotactic guidance of nerve growth cones. *Nature* **417**, 411–418

46. Loschinger, J., Weth, F., and Bonhoeffer, F. (2000) Reading of concentration gradients by axonal growth cones. *Phil. Trans. R. Soc. Lond. B Biol. Sci.* **355**, 971–982

47. Kastian, R. F., Minegishi, T., Baba, K., Saneyoshi, T., Katsuno-Kambe, H., Saranpal, S., *et al.* (2021) Shootin1a-mediated actin–adhesion coupling generates force to trigger structural plasticity of dendritic spines. *Cell Rep.* **35**, 109130

48. Katsuno, H., Toriyama, M., Hosokawa, Y., Mizuno, K., Ikeda, K., Sakumura, Y., *et al.* (2015) Actin migration driven by directional assembly and disassembly of membrane-anchored actin filaments. *Cell Rep.* **12**, 648–660

49. Inagaki, N., and Katsuno, H. (2017) Actin waves: origin of cell polarization and migration? *Trends Cell Biol.* **27**, 515–526

50. Baucum, A. J., 2nd, Brown, A. M., and Colbran, R. J. (2013) Differential association of postsynaptic signaling protein complexes in striatum and hippocampus. *J. Neurochem.* **124**, 490–501

51. Hou, H., Sun, L., Siddoway, B. A., Petralia, R. S., Yang, H., Gu, H., *et al.* (2013) Synaptic NMDA receptor stimulation activates PP1 by inhibiting its phosphorylation by Cdk5. *J. Cell Biol.* **203**, 521–535

52. Foley, K., McKee, C., Nairn, A. C., and Xia, H. (2021) Regulation of synaptic transmission and plasticity by protein phosphatase 1. *J. Neurosci.* **41**, 3040–3050

53. Higashiguchi, Y., Katsuta, K., Minegishi, T., Yonemura, S., Urasaki, A., and Inagaki, N. (2016) Identification of a shootin1 isoform expressed in peripheral tissues. *Cell Tissue Res.* **366**, 75–87

54. Minegishi, T., Uesugi, Y., Kaneko, N., Yoshida, W., Sawamoto, K., and Inagaki, N. (2018) Shootin1b mediates a mechanical clutch to produce force for neuronal migration. *Cell Rep.* **25**, 624–639.e6

55. Toriyama, M., Shimada, T., Kim, K. B., Mitsuba, M., Nomura, E., Katsuta, K., *et al.* (2006) Shootin1: a protein involved in the organization of an asymmetric signal for neuronal polarization. *J. Cell Biol.* **175**, 147–157

56. Gee, K. R., Sun, W. C., Bhalgat, M. K., Upson, R. H., Klaubert, D. H., Latham, K. A., *et al.* (1999) Fluorogenic substrates based on fluorinated umbelliferones for continuous assays of phosphatases and beta-galactosidases. *Anal. Biochem.* **273**, 41–48